ELSEVIER

Journal of Chromatography A, 668 (1994) 31–45

JOURNAL OF CHROMATOGRAPHY A

Application of a statistical geometrical theory to aqueous two-phase systems

Yue Guan[a,b], Timothy E. Treffry[a], Terence H. Lilley*[,b]

[a]*Department of Molecular Biology and Biotechnology, and Krebs Institute for Biomolecular Research, The University, Sheffield S10 2UH, UK*

[b]*Biothermodynamics Laboratory, Department of Chemistry, and Krebs Institute for Biomolecular Research, The University, Sheffield S3 7HF, UK*

Abstract

In a recent publication, we presented a novel theory based on a statistical geometric concepts which gave a simple analytical expression for the coexistence curves (binodals) of aqueous two-phase systems. In the present paper, this theory (which we term the binodal model) has been applied, with considerable success, to polymer + polymer and polymer + salt aqueous two-phase systems. For polyethylene glycol (PEG) + Dextran (Dex) aqueous two-phase systems, the binodal model gives satisfactory agreement with experiment when the molar mass ratio of Dex to PEG $\geq$ *ca.* 4. For PEG + salt aqueous two-phase systems, where the molar mass ratio of PEG to salt is almost invariably large, the binodal model works well. The model also explains the influence of both temperature and polymer molar mass on binodals and confirms the experimental observation found for some systems that under some circumstances the lower-molar-mass polymer can induce phase separation at lower concentrations than the polymer with the higher molar mass.

1. Introduction

Aqueous two-phase systems provide benign and non-destructive environments for bioseparation processes. Systems such as these are attractive in that they provide a means of separation which is, easy to manipulate, reliable in scaling-up, simple and effective in operation. A major objective of our recent work on aqueous two-phase systems is toward the establishment of soundly based, predictive methods for the determination of the system variables which give very efficient separation and purification of biomacromolecules under commercial conditions.

The prediction of the behaviour of aqueous systems is a notoriously difficult problem. Some approaches which have been used to solve problems associated with the formation of aqueous two-phase systems and/or protein partitioning behaviour in these systems are polymer lattice theories [1,2], the UNIQUAC and UNIFAC models [3–5], osmotic virial expansions [6], polymer scaling analyses [7] and the generalised means-spherical approximation [8].

Most of the protein partitioning models currently available are applicable only to very low protein concentrations, but any process using aqueous two-phase systems which could be applicable in an industrial situation would need to use high biomass loadings. We have recently demonstrated the feasibility of using aqueous two-phase partitioning to extract, from systems

* Corresponding author.

0021-9673/94/$07.00
SSDI 0021-9673(94)00002-Q

containing biomass loadings of up to 15% (w/v), the commercially important intracellular enzyme, penicillin acylase [9,10]. As well as introducing the problem of an extra insoluble phase when, for example, the protein concentration (or the total biomaterial concentration) is high enough for protein–protein molecular interactions to contribute significantly to the thermodynamic properties of these systems, perturbations of phase behaviour must also occur. Given, however, the hydrophilic nature of the protein surface, rather than having a system with two phase-forming components, in effect, such a system would now consist of three phase-forming components.

An aqueous two-phase system for protein separation contains at least four components, but molecular information on interactions between components can be obtained by studying some three-component systems, one of which is the aqueous two-phase system without the addition of biomacromolecules to be separated. Information of this nature is useful and applicable to systems containing both low and high concentrations of biomacromolecules. At very low protein concentrations, the contribution of protein to the formation of a two-phase system need not be considered since the molecular environment of the phase-forming components before and after the addition of protein is essentially unchanged. In contrast, at high total protein concentration, as mentioned above, the protein can also act as a phase-forming polymer and so initiate a redistribution of the primary phase-forming components with consequent perturbation of the phase diagram and it is the modified system which now controls the partitioning of the protein of interest.

In phase diagrams the axes give the concentrations of the phase-forming components and a curve, the binodal, separates the two-phase region, which is distal to the origin, from the single-phase region lying between the axes and the binodal. In a three-component system (solvent + two solutes), for any particular pair of solute concentrations leading to two phases in equilibrium, the concentrations of the solute components in each phase lie at two points on the binodal. A line connecting these points (the tie-line) must (because of material balance considerations) pass through a point on the phase diagram which represents the imaginary concentration of the phase-forming components in the bulk system: this point must divide the tie-line in the same proportion as the ratio of the masses of the phases. A necessary first step in quantifying the partitioning of a protein is the complete description of the phase diagram. At low protein concentrations, one of the "driving forces" for protein partitioning can be ascribed to the concentration of either of the phase-forming components. There are several ways to express this "driving force" such as the tie-line length [6] and the concentration difference of a phase-forming component between the two phases [11]. Our philosophy in dealing with problems on such systems has been that any adequate approach should be (i) consistent with thermodynamics, and (ii) applicable to both phase-forming components ("1" and "2") + water ternary systems and to phase-forming components ("1" and "2") + water + biomolecule quaternary systems. As mentioned above, although the Flory–Huggins theory, osmotic virial expansions, UNIQUAC and integral-equation approaches have been applied to these problems with some success, all have shortcoming when the complete calculation of phase diagrams is sought, or if protein distribution is to be predicted. However, notwithstanding the deficiencies of these approaches some useful and quite general empirical relationships of phase diagrams of aqueous two-phase systems have been suggested recently.

If we consider the application of the empirical Setchenow equation [12] (which can be related to osmotic virial expansions under restricted conditions [13]) to aqueous two-phase systems, we may write

$$\ln \frac{w_i^{\mathrm{T}}}{w_i^{\mathrm{B}}} = \beta_i + k_j^i (w_j^{\mathrm{B}} - w_j^{\mathrm{T}}) \qquad (1)$$

where k_j^i is the Setchenow salting-out coefficient of the ith component by the jth component, β_i is a constant accounting for the activity coefficient of the ith component in the coexisting phases,

$w_i^T(w_j^T)$ and $w_i^B(w_j^B)$ are the mass concentrations of species i (j) in the top and bottom phases, respectively. The correlation by Vainerman *et al.* [14] indicates that for aqueous two-phase systems the coefficient β_i is close to zero compared to the term $(w_i^B - w_i^T)$ and so we obtain the following expressions linking the compositions of the phase-forming components:

$$\ln \frac{w_1^T}{w_1^B} = \alpha_1(w_2^T - w_2^B) \quad (2a)$$

or

$$\ln \frac{w_2^T}{w_2^B} = \alpha_2(w_1^T - w_1^B) \quad (2b)$$

A somewhat unexpected feature is that the experimental information which is available indicates that Eqs. 2a and 2b are applicable to both polymer + polymer and polymer + salt aqueous two-phase systems [14]. Independently, Diamond and Hsu [15] obtained Eqs. 2a and 2b from the Flory–Huggins theory [16] and further compared them with a number of experimental results. However, the derivation used and the assumptions on which this is based are such that, at best, it could only apply to polymer + polymer aqueous two-phase systems and it is difficult to justify its use to systems containing salts. Using a different approach we have recently demonstrated [17] that one can also arrive at Eqs. 2a and 2b using what we call empirical "effective" osmotic virial coefficients for polymer + polymer aqueous two-phase systems but this approach has similar theoretical limitations regarding its application to systems containing electrolytes.

Even assuming the correctness of Eqs. 2a and 2b, they are insufficient to describe the phase diagram or even the binodal, and to get this some further relations are needed.

A novel approach [18], which we term the "binodal model," to the description of phase diagrams has been made very recently using the concepts of statistical geometry and, as a consequence, it has been shown that most of the binodals used in polymer + polymer aqueous two-phase systems can be described by

$$\ln\left(\langle V\rangle_{210}\frac{\rho N_A w_2}{\langle M\rangle_2}\right) + \langle V\rangle_{210}\frac{\rho N_A w_1}{\langle M\rangle_1} = 0 \quad (3)$$

where $\langle V\rangle_{210}$ is the effective excluded volume (EEV) of species 2 in the species 1 aqueous solution, ρ is the solution density, N_A is Avagadro's constant $\langle M\rangle_1$ and $\langle M\rangle_2$ are mean molar masses for species 1 and 2, and usually the root-mean-square average molar masses for polydisperse components are taken. One advantage of Eq. 3 over Eqs. 2a and 2b is that it describes the entire binodal using only one parameter which has a clearly defined physical meaning. An important feature of Eq. 3 is that Eqs. 2a and 2b can be derived from it, but the converse does not apply.

It is worth mentioning that although most of the existing theories or semiempirical treatments contain a logarithmic first term, they generally cannot be truncated to the form of the binodal model [17].

In the present paper we outline the theoretical bases of our binodal model and demonstrate situations where this model can be applied. Another objective of the present work is to collect most of the available phase diagram data for both polymer + polymer and polymer + salt aqueous two-phase systems to (i) determine the experimental validity of the binodal model and (ii) its range of suitability for different types of systems, and (iii) calculate and collect "effective excluded volume" parameters for different systems to guide subsequent engineering design of aqueous two-phase systems for bioseparation.

2. Theoretical aspects

A detailed description of the approach we have used to derive the binodal model has been given elsewhere [18] and in this section we simply outline a summary of the assumptions necessary to formulate this theory. We also, however, include some of the more mathematical details which were not stressed in the earlier paper.

Our analyses of the phase separation problem for polymer + polymer aqueous two-phase systems are based on the following assumptions:

(i) Molecules of the same species are distributed at random in a homogeneous phase.

(ii) On the coexistence curve, the structure of the solution is geometrically saturated [18] in terms of the sizes and shapes of all of the molecules in the system.

(iii) The existence of molecular interactions does not change the nature of this random molecular distribution and, on the coexistence curve, their effects are exhibited simply as an adjustment of the average distances between the unlike molecular centres.

Assumption i can include situations where specific association effects at the molecular level are very strong if the aggregated species are taken to be the primary components. For example, for a semi-ordered liquid phase such as a micellar solution [19], one must regard the associated "polymers" as the solutes and it is these to which the random distribution assumption is applied. In making assumption ii, we have indicated that the solution structures before and after (or from) phase separations are different. Before phase separation (*i.e.* in the one-phase region), solute molecules are separated so that additional solute molecules can still be inserted into the free space which is present. At the point of phase separation, the solute molecules are now so closely packed that the solution is not able to accept any additional solute molecules and when the total solute concentration is increased, what happens is the formation of two geometrically saturated yet structurally quite different solutions. The further the system is from the critical point (the plait point), the more different are the structures of these two saturated solutions. Assumption iii recognises an important phenomenon which has been verified by computer simulations [20], *viz.* that molecular interactions are not always necessary for the occurrence of phase separation.

For an aqueous solution containing two very soluble solutes (or indeed any other binary solute solution in a "good" solvent), when the steric hindrance of the water molecules to the solutes is small compared with that between the two solute species (under these circumstances we say the two solute components are "geometrically incompatible"), we can regard the system as a pseudo-binary system. To model such a system we consider the size distribution of convex "holes" in a network of species i which could possibly accommodate molecules of type j. If we let ν_i and ν_j be the corresponding molecular number densities, φ_i the probability density function of finding holes with a volume at least V in the molecular centre network formed by species i, then it has been shown [18] that

$$\varphi_i(V)\,\mathrm{d}V = \lambda_{i(01)}(V)\,\mathrm{d}V \int_0^\infty \varphi(x)\,\mathrm{d}x \tag{4}$$

where $\lambda_{i(01)}(V)$ is a function which only depends on the hole size in the molecular centre network of species i, $\lambda_{i(01)}(V)\,\mathrm{d}V$ is the conditional probability that the infinitesimal shell of volume $\mathrm{d}V$ contains one molecular centre of species i when there is no molecular centre of species i in the volume V (see Fig. 1). According to this definition, when $\nu_i \neq 0$, $\lambda_{i(01)}(V)\,\mathrm{d}V$ must always adopt positive values and must not be a decreasing monotonic function, *i.e.*

$$\lambda_{i(01)}(V_2)\,\mathrm{d}V_2 \geq \lambda_{i(01)}(V_1)\,\mathrm{d}V > 0 \quad (V_2 > V_1) \tag{5}$$

Using Eq. 5, we obtain

$$\int_0^\infty \lambda_{i(01)}(V)\,\mathrm{d}V = \infty\,, \tag{6}$$

which will be used later. Solving Eq. 4 gives

$$\varphi_i(V) = \frac{\varphi_i(0)}{\lambda_{i(01)}(0)} \cdot \lambda_{i(01)}(V) \exp\left[-\int_0^V \lambda_{i(01)}(x)\,\mathrm{d}x\right] \tag{7}$$

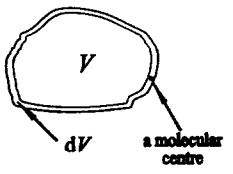

Fig. 1. Diagram illustrating a convex cavity of volume V in a network of species "i" where only single molecular centre of component i occupies the infinitesimal shell of volume $\mathrm{d}V$ around this cavity.

Substituting Eq. 7 into the following restriction to $\varphi_i(V)$:

$$\int_0^\infty \varphi_i(V)\,dV = 1 \tag{8}$$

Noting the following relation:

$$d\exp\left[-\int_0^V \lambda_{i(01)}(x)\,dx\right] = -\lambda_{i(01)}(V)\,dV \exp\left[-\int_0^V \lambda_{i(01)}(x)\,dx\right] \tag{9}$$

and Eq. 6, we get: $\varphi_i(0)/\lambda_{i(01)}(0) = 1$ and so Eq. 7 becomes

$$\varphi_i(V) = \lambda_{i(01)}(V)\exp\left[-\int_0^V \lambda_{i(01)}(x)\,dx\right] \tag{10}$$

Using Eq. 10, the probability of finding interstitial spacings V adjacent to molecules of species i is given by

$$P(\underline{V} \geq V) = \int_V^\infty \varphi_i(V)\,dV = \exp\left[-\int_0^V \lambda_{i(01)}(x)\,dx\right] \tag{11}$$

where $P(\underline{V} \geq V)$ is the probability of finding a cavity of volume at least V. The function $\lambda_{i(01)}(V)$ may be determined by the following further restriction to $\varphi_i(V)$:

$$\int_0^\infty V\varphi_i(V)\,dV = \frac{1}{\nu_i} \tag{12}$$

Substituting Eq. 10 into Eq. 12 gives

$$\int_0^\infty \exp\left[-\int_0^V \lambda_{i(01)}(x)\,dx\right] dV = \frac{1}{\nu_i} \tag{13}$$

If, since in our model the molecular distribution is random, we consider, for guidance, the random spheres model where molecules are mutually penetrable [21], we expect:

$$\lambda_{i(01)}(V) = \text{constant} \tag{14}$$

and by insertion of Eq. 14 into Eq. 13, we determine $\lambda_{i(01)} = 1/\nu_i$ and so Eq. 11 becomes

$$P(\underline{V} \geq V) = \exp(-V\nu_i) \tag{15}$$

However, molecular repulsions become ever more significant and the deviations from completely random behaviour become greater as the distance between molecular centres becomes smaller. If for mathematical simplicity and for purposes of illustration a linear repulsion is assumed, *i.e.*

$$\lambda_{i(01)} = \gamma V \tag{16}$$

where γ is a constant, then insertion of Eq. 16 into Eq. 13 leads to $\lambda_{i(01)}(V) = \pi\nu_i^2 V/2$. Correspondingly, Eq. 11 becomes

$$P(\underline{V} \geq V) = \exp\left(-\frac{\pi}{4}\cdot\nu_i^2 V^2\right) \tag{17}$$

We conclude from this that Eq. 15 is a reasonable approximation to the real systems when the minimum hole size is relatively large and Eq. 17 is a plausible approximation when this hole size is relatively small. For the particular systems which we are considering here, since the size of the cavity is at least that of the effective excluded volume (which is greater than the molecular size of either species), Eq. 15 should be a good approximation.

Combination of Eq. 15 with assumption ii, for the pseudo-binary system i–j–0 [18] allows us to write:

$$e^{-V_{ji0}\nu_i} = V_{ji0}\nu_j + f_{ji0} \tag{18}$$

where V_{ji0} is the effective excluded volume of species j in the species i aqueous solution, and is the minimum volume in the molecular centre network of species i which holds an individual j molecule, and f_{ji0} represents the volume fraction of unfilled effective available volume after tight packing of species j in the network of species i aqueous solution.

We now define a new parameter, R, the ratio of molecular masses of the two phase-forming components, as

$$R = \frac{\langle M\rangle_j}{\langle M\rangle_i} \tag{19}$$

Usually, for most systems of interest [*e.g.*, the phase-forming components are polyethylene glycol (PEG) + Dextran (Dex) or PEG + salt], the value of R is greater than unity. It should be noted that as R becomes large f_{ji0} approaches

zero, and consequently, the coexistence curves of most aqueous two-phase systems may be simply expressed as:

$$\exp(-V_{ji0}\nu_i) = V_{ji0}\nu_j \tag{20}$$

3. The use of Eq. 20

There are usually two types of aqueous two-phase systems currently adopted for bioseparations of biomacromolecules, *viz.* polymer + polymer and polymer + salt systems. For polymer + polymer systems, the difference of the densities of the two equilibrated phases is so small that one can neglect this difference in modelling the phase diagram. For polymer + salt systems, however, this difference should be considered even when allowing for the experimental inaccuracy in determining the phase diagram. Because of this, there are two resultant expressions in the application of Eq. 20 to aqueous two-phase systems.

3.1. Polymer + polymer aqueous two-phase systems

Using the root-mean-square molar mass ($\langle M_{\mathrm{rms}}\rangle$) for a polydisperse species and since the densities along the binodal are almost the same (the density difference between the two phases of PEG + Dex systems is less than 10^{-5} kg m^{-3} [22]), we can therefore create a new parameter the average scaled EEV ($\langle V^*\rangle_{ji0} = N_{\mathrm{A}}\langle \rho V_{ji0}\rangle$) and using this, the following expression results from Eq. 20:

$$\ln\left(\langle V^*\rangle_{210}\frac{w_2}{\langle M_{\mathrm{rms}}\rangle_2}\right) + \langle V^*\rangle_{210}\frac{w_1}{\langle M_{\mathrm{rms}}\rangle_1} = 0 \tag{21}$$

For PEG + Dex aqueous two-phase systems, species 1 and 2 refers to PEG and Dex, respectively.

3.2. Polymer + salt aqueous two-phase systems

The coexistence of electrolytes and the non-ionic polymers necessarily makes the molecular interactions in solutions more complex and the assumption of a completely random distribution must be doubtful since one would expect some degree of correlation between the ions of the electrolyte [23]. However, the exponential law of Eq. 15 is still expected to be a useful approximation for polymer molecules. We do not know why the approach adopted works as well as it does for systems containing electrolytes and for this reason we prefer to consider the following expression to be semi-empirical:

$$\ln\left(\langle V^{**}\rangle_{210}\frac{\rho w_2}{\langle M_{\mathrm{rms}}\rangle_2}\right) + \langle V^{**}\rangle_{210}\frac{\rho w_1}{\langle M_{\mathrm{rms}}\rangle_1} = 0 \tag{22}$$

In this, $\langle V^{**}\rangle_{ji0} = \rho N_{\mathrm{A}}\langle V_{ji0}\rangle$ is taken as the average scaled EEV. For PEG + salt aqueous two-phase systems, species 1 and 2 denotes salt and PEG respectively.

Uses of Eqs. 21 and 22 are examined and discussed briefly below.

4. Results and discussion

One of the major objectives of the present work is to compare our theoretical expressions with experimental phase diagram.

It is true that polymers are complex molecules and their solution behaviour has been represented in different ways depending on the concentration regime considered. For aqueous two-phase systems, the concentrations of the polymers are in the "semi-dilute" region or perhaps approaching a crossover domain [24]. Although these different physical situations are not detailed in our model, the links of the binodal model to these have been indicated [18]. We have found Fig. 6 of ref. 18) that the change of the EEV with Dextran molar mass in PEG + Dex aqueous two-phase systems is marked at lower Dextran molar masses, but increasingly less marked at higher molar masses. This observation is in accordance with the physical model on which a recent theoretical analysis [7] is based. We would expect from the assumptions

made in the formulation of the theory, that for systems containing high-molar-mass polymers in the concentration region considered, the polymer molecules will form an entangled network rather than exist as identifiable polymer coils. The consequence of this is that the solution properties should be little influenced by the polymer molar mass at high molar masses but we would expect some influence at low molar masses. Within the limitations imposed by the model formulation it is therefore able to reflect different scale lengths. It is appreciated that the model used is oversimplified and cannot represent in detail all aspects of the molecular idiosyncrasies of all polymers. Comparisons with experimental information indicate that the theory is robust, but, undoubtedly, the EEV acts to some extent as a "catch-all" and must reflect, to some extent, "chemical" as distinct from geometric properties of the polymers.

For PEG + Dex aqueous two-phase systems, the phase diagram data obtained by Forciniti *et al.* [25], Diamond and Hsu [26], and Albertsson [27] have been correlated using Eq. 21 and the results obtained are given in Tables 1–3. It is clear from the information presented that the data from all of these sources, when the molecular mass ratio, R, is greater than *ca.* 4, is satisfactorily represented by Eq. 21. However, when R is less than this value, significant deviations of experimental results sometimes are evident. We can therefore conclude that for PEG + Dex aqueous two-phase systems, when $R > ca.$ 4 the binodal model works well.

A feature of the results given in Tables 1–3 is that the calculated EEVs from different sources but for seemingly identical PEG + Dex pairs, at similar temperatures (*e.g.*, 293 and 298 K), are sometimes very different. Some of the variation may be due to differing experimental conditions in different laboratories but the major contributions to the variations most probably arise from variations in the molar masses and polydispersity of the phase-forming polymers used. These variations however have a much less pronounced effect with PEG than with Dex. The variability

Table 1
Calculated effective excluded volumes ($\langle V^* \rangle_{\text{Dex-PEG-H}_2\text{O}}$) in PEG + Dextran aqueous two-phase systems at 298 K, obtained by fitting the experimental data [25] to Eq. 21

PEG + Dex aqueous systems[a]	$10^2 \times \langle V^*_{\text{Dex-PEG-H}_2\text{O}} \rangle$ (kg mol^{-1})	r	n	R
PEG 20 000 + Dex 17[b]	2.354	0.865	8	0.8
PEG 10 000 + Dex 17[b]	1.344	0.902	8	1.5
PEG 20 000 + Dex 19[b]	4.397	0.922	8	1.6
PEG 6000 + Dex 17	0.806	0.948	7	2.9
PEG 10 000 + Dex 19[b]	2.630	0.962	8	3.0
PEG 20 000 + Dex 37	7.191	0.958	8	3.3
PEG 4000 + Dex 17	0.614	0.968	8	4.1
PEG 6000 + Dex 19	1.393	0.988	8	5.9
PEG 10 000 + Dex 37	4.316	0.989	8	6.2
PEG 20 000 + Dex 48	9.426	0.987	8	6.87
PEG 4000 + Dex 19	1.025	0.995	8	8.1
PEG 6000 + Dex 37	2.308	0.986	8	12.2
PEG 10 000 + Dex 48	4.934	0.961	8	12.7
PEG 4000 + Dex 37	1.499	0.997	8	17.0
PEG 6000 + Dex 48	2.621	0.970	8	25.1
PEG 4000 + Dex 48	1.781	0.977	8	34.8

[a] Root-mean-square molar masses were used as the average molar masses and, for PEG 4000, PEG 6000, PEG 10 000, PEG 20 000, Dex 17, Dex 19, Dex 37 and Dex 48, they were 3951, 5476, 10 809, 20 038, 15 996, 32 017, 66 983 and 13 657, respectively.
[b] Phase diagrams for these systems are not given.

Table 2
Calculated effective excluded volumes ($\langle V^* \rangle_{Dex-PEG-H_2O}$) in PEG + Dextran aqueous two-phase systems at 277 K, obtained by fitting the experimental data [26] to Eq. 21

PEG + Dex aqueous systems[a]	$10^2 \times \langle V^*_{Dex-PEG-H_2O} \rangle$ (kg mol^{-1})	r	n	R
PEG 20 000 + Dex T40[b]	3.784	0.923	8	1.6
PEG 20 000 + Dex T70[b]	5.447	0.952	14	2.6
PEG 8000 + Dex T40	1.832	0.977	10	3.9
PEG 8000 + Dex T70	2.624	0.996	10	6.6
PEG 3400 + Dex T40	0.830	0.995	8	9.2
PEG 3400 + Dex T70	1.078	0.993	8	15.5
PEG 20 000 + Dex T500	14.696	0.983	8	17.2
PEG 8000 + Dex T500	6.129	0.978	8	43.1
PEG 3400 + Dex T500	2.279	0.991	8	101.3

[a] The average molar masses of PEG 3400, PEG 8000 and PEG 20 000 were 3400, 8000 and 20 000, respectively. The root-mean-square average molar masses used for Dex T40, T70 and T500 were 31 319, 52 654 and 344 586, respectively.
[b] Phase diagrams for these systems are not given.

of molar mass and polydispersity from different manufacturers and different batches is the main obstacle to achieving a general design approach to polymer + polymer aqueous two-phase systems using parameters such as the EEV. It has ben suggested [17] that at the outset of experiments in which an aqueous two-phase system is to be used, the EEV should be measured using, for example, the experimentally simple "turbidity" approach [27] to characterise the particular system studied. The suitability of this experimental approach for both types of aqueous two-phase systems has been demonstrated [28]. It is possible that a series of batches of the polymers

Table 3
Calculated effective excluded volumes ($\langle V^* \rangle_{Dex-PEG-H_2O}$) in PEG + Dextran aqueous two-phase systems, obtained by fitting the experimental data [27] to Eq. 21

PEG + Dex aqueous systems[a]	$10^2 \times \langle V^*_{Dex-PEG-H_2O} \rangle$ (kg mol^{-1})	r	n	R
PEG 20 000 + Dex D17 at 293 K[b]	2.722	0.894	12	1.3
PEG 6000 + Dex D17 at 273 K	1.564	0.954	8	2.9
PEG 6000 + Dex D17 at 293 K	1.527	0.959	14	2.9
PEG 6000 + Dex D24 at 293 K	2.069	0.993	10	5.1
PEG 4000 + Dex D17 at 293 K	0.742	0.975	8	5.8
PEG 6000 + Dex D37 at 273 K	3.976	0.991	10	10.4
PEG 6000 + Dex D37 at 293 K	3.552	0.995	8	10.4
PEG 6000 + Dex D48 at 273 K[b]	5.811	0.995	10	36.0
PEG 6000 + Dex D48 at 277 K	6.650	0.992	10	36.0
PEG 6000 + Dex D48 at 293 K	4.967	0.987	14	36.0
PEG 6000 + Dex D68 at 273 K	7.337	0.993	8	37.3
PEG 6000 + Dex D68 at 293 K	6.033	0.986	10	37.3
PEG 4000 + Dex D48 at 273 K	2.534	0.996	10	45.0
PEG 4000 + Dex D48 at 293 K	1.932	0.989	10	47.7

[a] Average molar masses for PEG 4000, PEG 6000 and PEG 20 000 were 4000, 8000 and 17 500, respectively. Those for Dex D17, D24, D37, D48 and D68 were 23 000, 40 500, 83 000, 180 000 and 280 000, respectively.
[b] Phase diagram for this system is not given.

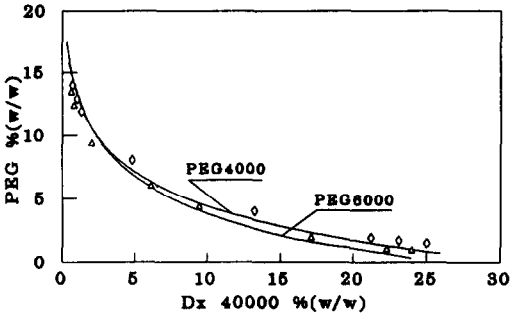

Fig. 2. Comparison of experimental binodals [25] for PEG 4000–Dextran (Dx) 40 000–water (◇) and PEG 6000–Dextran 40 000–water (△) systems at 298 K with those calculated (–) from Eq. 21.

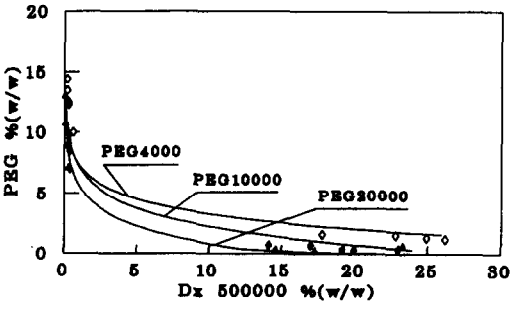

Fig. 4. Comparison of experimental binodals [25] for PEG 4000–Dextran (Dx) 500 000–water (◇), PEG 10 000–Dextran 500 000–water (◆) and PEG 20 000–Dextran 500 000–water (▲) systems at 298 K with those calculated (–) from Eq. 21.

obtained from a given manufacturer, might well be consistent in their properties. This would be fortunate but should always be checked.

Calculated and experimental binodals of a number of PEG + Dex aqueous two-phase systems are shown in Figs. 2–10. Without exception, for all of the experimental data considered (including systems containing salt, see later), we find that for different pairs of phase-forming components of similar chemical nature, the greater the polymer molar mass, the greater is the EEV: this is consistent with the physical meaning of the EEV.

From the results shown in Figs. 2–10 we find another important feature of the binodal model is that it reflects influences of both polymer molar mass and temperature on shifts in the

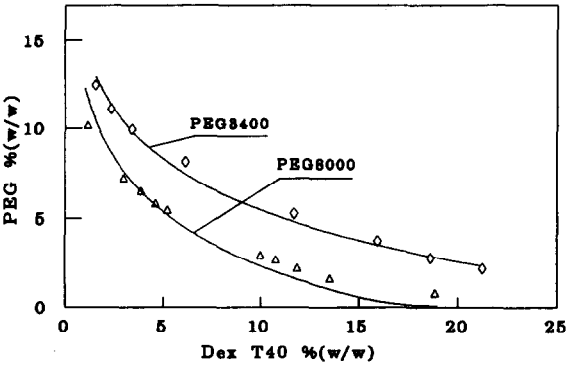

Fig. 5. Comparison of experimental binodals [26] for PEG 3400–Dextran T40–water (◇) and PEG 8000–Dextran T40–water (△) systems at 295 K with those calculated (–) from Eq. 21.

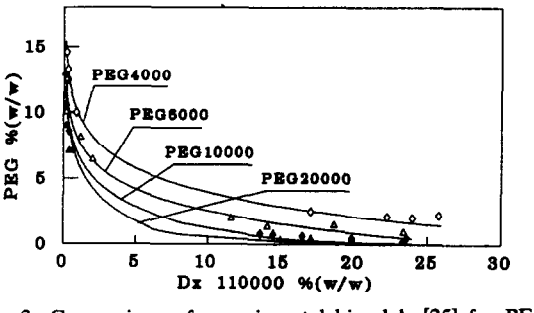

Fig. 3. Comparison of experimental binodals [25] for PEG 4000–Dextran (Dx) 110 000–water (◇), PEG 6000–Dextran 110 000–water (△), PEG 10 000–Dextran 110 000–water (◆) and PEG 20 000–Dextran 110 000–water (▲) systems at 298 K with those calculated (–) from Eq. 21.

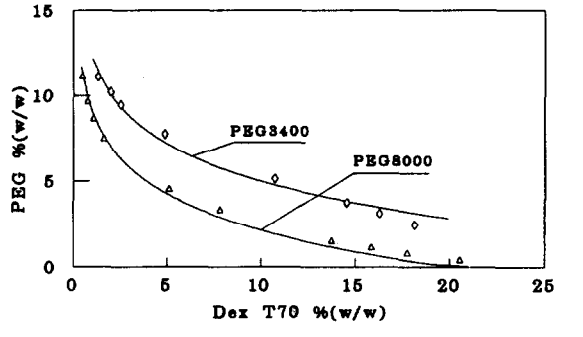

Fig. 6. Comparison of experimental binodals [26] for PEG 3400–Dextran T70–water (◇) and PEG 8000–Dextran T70–water (△) systems at 295 K with those calculated (–) from Eq. 21.

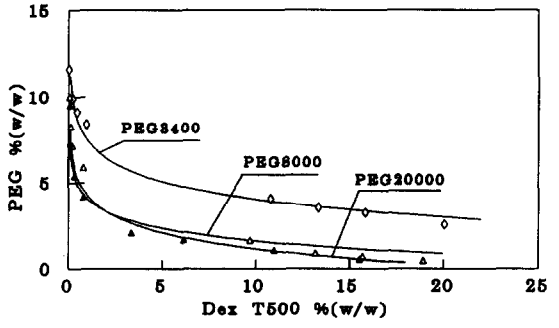

Fig. 7. Comparison of experimental binodals [26] for PEG 3400–Dextran T500–water (◇), PEG 8000–Dextran T500–water (△) and PEG 20 000–Dextran T500–water (▲) systems at 295 K with those calculated (–) from Eq. 21.

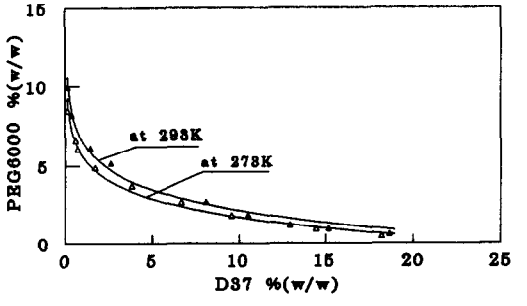

Fig. 8. Comparison of experimental binodals [27] for PEG 6000–Dextran D37–water systems at 293 K (▲) and at 273 K (△) with those calculated (–) from Eq. 21.

binodal. Two empirical concepts, which have been established for many years and are based primarily on experimental observations, are (i)

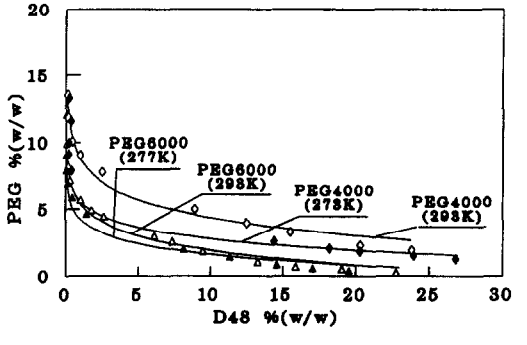

Fig. 9. Comparison of experimental binodals [27] with PEG 4000–Dextran D48–water systems at 293 K (◇) and at 283 K (◆) and PEG 6000–Dextran D48–water systems at 293 K (△) and at 277 K (▲) with those calculated (–) from Eq. 21.

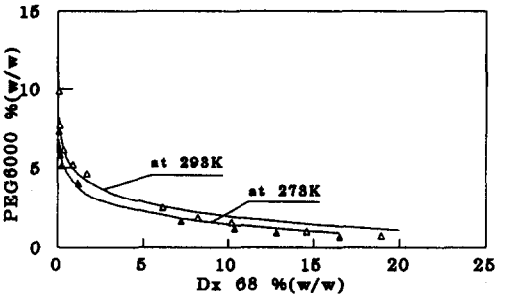

Fig. 10. Comparison of experimental binodals [27] for PEG 6000–Dextran (Dx) 68–water systems at 293 K (△) and 273 K (▲) with those calculated (–) from Eq. 21.

the higher the temperature the higher the concentration of polymers needed for phase separation and (ii) the higher the molar mass the lower the concentration of polymers needed for phase separation (see, *e.g.*, refs. 27, 29 and 30).

The first of these two concepts is completely in accordance with the predictions of the binodal model in that for a given polymer + polymer system, if the temperature is increased, then the EEV necessarily will decrease, resulting in a consequent perturbation of the coexistence curve away from the axes. In other words, for a fixed pair of polymers at higher temperatures, higher concentrations of the phase-forming polymers are always required for phase separation. It should perhaps be mentioned that, because of experimental problems at the extremes of coexistence curves, it is often difficult to delineate the exact relative positions of the curves (see, *e.g.*, Figs. 8 and 10).

The second of the empirical observations is consistent with the binodal model but is not a necessary condition of it. If the concentrations of the phase-forming solutes are expressed as molecular number densities then one can categorically state for two binary solute systems in which the molar mass of one of the solutes is fixed but the molar mass of the other solute varies, that the system with the lower-molar-mass solute will have its coexistence curve more distance from the axes than the higher-molar-mass solute containing system. However, usually phase compositions are expressed using mass fraction (or a similar scale) and depending upon the molar

masses it is possible for overlap of coexistence curves to occur when such scales are used. The EEV is related to the molecular size of both phase-forming components. When the molar mass ratio of the phase-forming components is large, a change in molar mass of the larger sized species will significantly alter the EEV whereas a change of the smaller sized species will have a lesser effect on the coexistence curve. As observed in Figs. 2, 3, 4, 7 and 9, for PEG + Dex aqueous two-phase systems when the molar mass of the larger sized species (Dex) is constant, the experimental evidence for binodal overlap with PEG of varying molar masses is unclear. In contrast, as shown in Figs. 11 and 12, when the molar mass of PEG is kept constant but that of Dex varies, binodal overlap obviously occurs.

As was mentioned above, changing the temperature leads to a change in the EEV and several examples illustrating this in polymer + polymer aqueous two-phase systems are given in Table 3. It is also possible to perturb the EEV, without changing the molar masses of the phase-forming polymers, by for example, the addition of a small amount of low-molar-mass additives, such as a salt or urea [30,31]. Changes in the EEV can also occur, with consequent changes in the phase diagrams, by derivatisation of the polymer(s).

A considerable amount of high-quality and

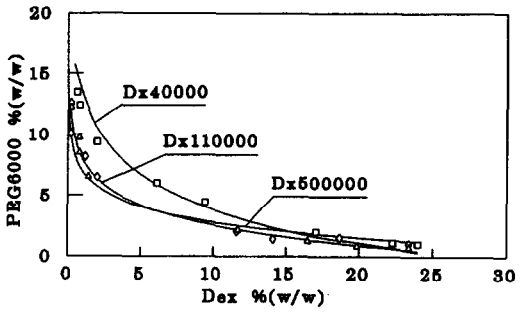

Fig. 11. Comparison of experimental binodals [25] for PEG 6000–Dex–water systems at 298 K, where the molecular mass of the PEG is fixed and those of Dex vary, with those calculated (–) from Eq. 21. Experimental results: □ = PEG 6000 + Dextran (Dx) 40 000 system; ◇ = PEG 6000 + 110 000 system; △ = PEG 6000 + Dextran 500 000 system.

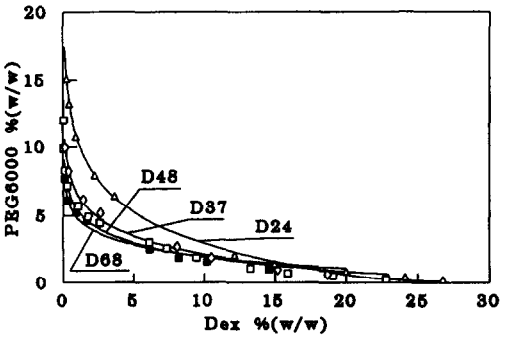

Fig. 12. Comparison of experimental binodals [27] for PEG 6000–Dex–water systems at 293 K, where the molecular mass of the PEG is fixed and those of Dex vary, with those calculated (–) from Eq. 21. Experimental results: ■ = PEG 6000 + Dextran D68 system; □ = PEG 6000 + Dextran D48 system; ◇ = PEG 6000 + Dextran D37 system; △ = PEG 6000 + Dextran D24 system.

comprehensive data on PEG + salt systems has recently been reported [32] and we have treated these using the binodal model. The results obtained are presented in Table 4 and shown in Figs. 13–17. It is apparent that the binodal model (Eq. 22), usually gives a satisfactory description of the experimentally determined binodals of polymer + salt aqueous two-phase systems. The molar mass ratio restriction on the binodal model seldom applies and generally since the molar mass ratio for this type of two-phase system is almost invariably rather high, polymer molecules would tend to be close packed in aqueous salt solutions [18]. One of the clear conclusions which is evident from Table 4 is that for each of the salt-containing systems investigated, as the molar mass of the PEG increases, so too does the EEV. This is in accordance with the binodal model. It seems quite apparent from the information shown in Figs. 14–17 that for PEG + salt systems binodal overlaps do occur. This is the feature which was commented on above when polymer + polymer systems were considered and now, largely because of the great molar mass disparity between the polymer and the salt and the variation in the larger sized species PEG, the non-monotonic shift of coexistence curves with polymer molar mass is very evident. In contrast to the polymer + polymer systems, where in the usual

Table 4
Calculated effective excluded volumes ($\langle V^{**} \rangle_{PEG-salt-H_2O}$) in PEG + salt aqueous two-phase systems at 298 K, obtained by fitting the experimental data [32] to Eq. 22

PEG + salt aqueous systems[a]	$10^7 \times \langle V^{**}_{PEG-salt-H_2O} \rangle$ ($m^3\ mol^{-1}$)	r	n	R
PEG 1000 + $MgSO_4$	1.777	0.994	8	9.1
PEG 3350 + $MgSO_4$	3.925	0.980	8	27.4
PEG 8000 + $MgSO_4$	5.500	a	10	73.5
PEG 1000 + K_3PO_4 at pH 8.0[b]	1.869	0.997	8	6.5
PEG 8000 + K_3PO_4 at pH 8.0[b]	7.400	0.975	12	52.4
PEG 1000 + Na_2CO_3	1.905	0.996	10	10.4
PEG 3350 + Na_2CO_3	2.480	0.998	6	31.1
PEG 8000 + Na_2CO_3	8.770	0.990	8	83.5
PEG 1000 + $(NH_4)_2SO_4$	1.387	0.995	8	8.3
PEG 8000 + $(NH_4)_2SO_4$	5.733	0.993	8	67.0
PEG 1000 + Na_2SO_4	1.994	0.997	10	7.7
PEG 3350 + Na_2SO_4	3.804	0.981	8	23.2
PEG 8000 + Na_2SO_4	5.557	0.995	10	62.3

[a] The root-mean-square-average molar masses were used for the average molar masses of PEG and for PEG 1000, PEG 3350 and PEG 8000 they were 1100, 3299 and 8848, respectively [32].

[b] For systems containing K_2HPO_4 and KH_2PO_4 the fractions of phosphate species ($x_{K_2HPO_4}$, $x_{KH_2PO_4}$) were determined using the Henderson–Hasselbach equation in association with the well documented pK_a of $H_2PO_4^-$. The mean molar mass of the phosphate was obtained by $\langle M \rangle_{phosphate} = M_{K_2HPO_4} x_{K_2HPO_4} + M_{KH_2PO_4} (1 - x_{K_2HPO_4})$, where $M_{K_2HPO_4}$ and $M_{KH_2PO_4}$ are the molar masses of K_2HPO_4 and KH_2PO_4, respectively.

composition ranges, as the molar mass of one of the polymer is increased the coexistence curve moves towards the axes, for polymer + salt systems as the molar mass of the polymer is increased either enhanced or diminished phase separation can occur. At the cross-over point

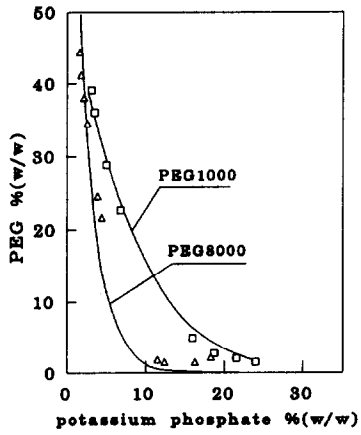

Fig. 13. Comparison of experimental binodals [32] for PEG 1000–potassium phosphate–water (□) and PEG 8000–potassium phosphate–water (△) systems at pH 8.0 and 298 K with those calculated (–) from Eq. 22.

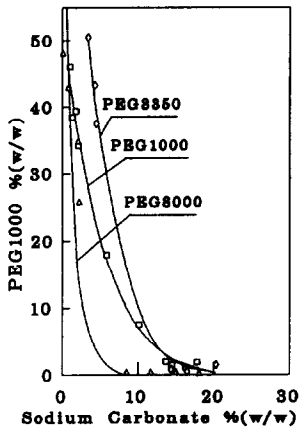

Fig. 14. Comparison of experimental binodals [32] for PEG 1000–Na_2CO_3–water (□), PEG 3350–Na_2CO_3–water (◇) and PEG 8000–Na_3Co_3–water (△) at 298 K with those calculated (–) from Eq. 22.

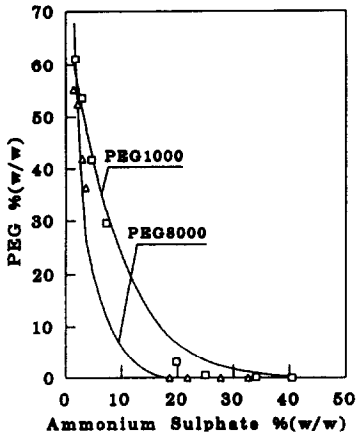

Fig. 15. Comparison of experimental binodals [32] for PEG 1000–$(NH_4)_2SO_4$–water (□) and PEG 8000–$(NH_4)_2SO_4$–water (△) systems at 298 K with those calculated (–) from Eq. 22.

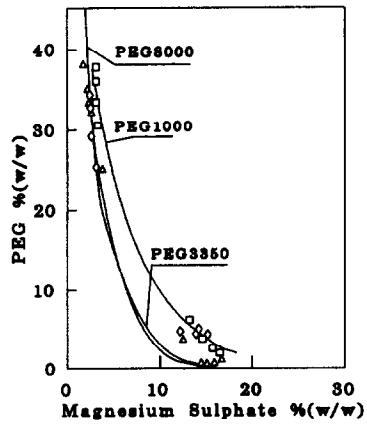

Fig. 17. Comparison of experimental binodals [32] for PEG 1000–Na_2SO_4–water (□), PEG 3350–Na_2SO_4–water (◇) and PEG 8000–Na_2SO_4–water (△) systems at 298 K with those calculated (–) from Eq. 22.

obviously no change in phase separation occurs with change in molar mass.

In the treatment of polymer + salt aqueous two-phase systems, the disadvantage of using Eq. 22 to predict the binodal is that a means of estimating the change of solution density along the binodal is needed. In order to obtain a simple expression for the polymer + salt aqueous two-phase systems, a tentative empirical approach for the present situation may be the use of Eq. 21. Tables 5 and 6 list the correlation of some PEG + phosphate binodals determined by Lei *et al.* [33] and Albertsson [27], and in these $N_A\langle\rho V_{\text{polymer-salt}}\rangle$ is used to represent the apparent EEV. It can be seen that although the correlation coefficients are somewhat reduced for the data reported by Albertsson [27], the approach is quite satisfactory for the binodals determined by Lei *et al.* [33]. From Table 5 it is apparent that for molar mass ratios greater than approximately 4 Eq. 21 gives satisfactory representations of the experimental binodals of PEG + phosphate systems. It would seem therefore that the application of Eq. 21 to polymer + salt aqueous two-phase systems should be satisfactory if this condition is met.

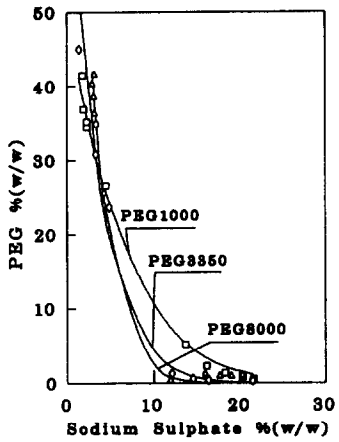

Fig. 16. Comparison of experimental binodals [32] for PEG 1000–$MgSO_4$–water (□), PEG 3350–$MgSO_4$–water (◇) and PEG 8000–$MgSO_4$–water (△) systems at 298 K with those calculated (–) from Eq. 22.

It was mentioned earlier that the application of binodal model to polymer + salt aqueous two-phase systems is semi-empirical, and there are some obvious theoretical difficulties. As an example as shown in Table 6, the influence of temperature on the EEV is different to that observed in polymer + polymer aqueous two-phase system in that for polymer + salt aqueous two-phase systems increase in temperature increases the EEV. It is our intention to study the

Table 5
Calculated effective excluded volumes ($\langle V^* \rangle_{PEG-salt-H_2O}$) in PEG + salt aqueous two-phase systems at 277 K, obtained by fitting the experimental data [33] to Eq. 21

PEG + salt aqueous systems[a]	$10^7 \times \langle V^*_{PEG-salt-H_2O} \rangle$ (kg mol^{-1})	r	n	R
PEG 400 + potassium phosphate at pH 7	0.880	0.979	8	2.7
PEG 600 + potassium phosphate at pH 7	1.240	0.990	8	4.0
PEG 1000 + potassium phosphate at pH 7	1.795	0.998	8	6.6
PEG 1500 + potassium phosphate at pH 7	2.415	0.999	8	10.0
PEG 3400 + potassium phosphate at pH 6	3.215	0.997	8	24.6
PEG 3400 + potassium phosphate at pH 7	3.865	0.994	8	22.6
PEG 3400 + potassium phosphate at pH 8	4.558	0.999	8	20.1
PEG 3400 + potassium phosphate at pH 9.2	4.616	0.999	8	19.6
PEG 8000 + potassium phosphate at pH 7	6.148	0.990	8	53.1
PEG 20 000 + potassium phosphate at pH 7	8.375	0.997	8	132.6

[a] The nominal masses were used for the PEGs. The average molar masses of phosphates were obtained as given in the footnote to Table 4.

behaviour of salt-containing systems in more detail, both from experimental and theoretical viewpoints.

5. Conclusions

Eqs. 21 and 22, which are based on a statistical geometrical theory, can represent both polymer + polymer or polymer + salt aqueous two-phase systems. The establishment of the binodal model represents a major step in the quantitative description of aqueous two-phase systems and biomacromolecular partitioning in these systems. In practice, given the marked influence of polymer polydispersity on the binodals of polymer + polymer aqueous two-phase systems and the variation of this between manufacturers and between batches, the preliminary determination of the parameter, the EEV, is recommended. For polymer + salt aqueous two-phase systems, the value of the EEV varies little

Table 6
Calculated effective excluded volumes ($\langle V^* \rangle_{PEG-salt-H_2O}$) in PEG + phosphate aqueous two-phase systems, obtained by fitting the experimental data [27] to Eq. 21

PEG + salt aqueous systems[a]	$10^6 \times \langle V^*_{PEG-salt-H_2O} \rangle$ (kg mol^{-1})	r	n	R
PEG 1540 + potassium phosphate at 293 K	2.388	0.994	8	9.7
PEG 4000 + potassium phosphate at 273 K	3.736	0.979	8	23.8
PEG 4000 + potassium phosphate at 293 K	4.021	0.972	12	23.8
PEG 6000 + potassium phosphate at 273 K	5.363	0.972	8	50.5
PEG 6000 + potassium phosphate at 293 K	5.656	0.979	8	50.5
PEG 20 000 + potassium phosphate at 293 K	6.809	0.988	6	110.4

[a] The average molar masses for PEG 1540, PG 4000, PEG 6000 and PEG 20 000 were 1540, 3774, 8000 and 17 500, respectively. The average molar masses of the phosphate used here were obtained as given in the footnote to Table 4.

for PEGs with molecular masses less than 10 000 for a given salt and at a given pH, and so such preliminary experimentation is unnecessary.

6. Acknowledgement

This work was supported by the Science and Engineering Research Council under Grant No. GR/G19824.

7. References

[1] D.E. Brooks, K.A. Sharp and D. Fisher, in H. Walter, D.E. Brooks and D. Fisher (Editors), *Partitioning in Aqueous Two-Phase Systems*, Academic Press, Orlando, FL, 1985, Ch. 2, p. 11.
[2] J.N. Baskir, T.A. Hatton and U.W. Suter, *Macromolecules*, 20 (1987) 1300.
[3] C.H. Kang and S.I. Sandler, *Fluid Phase Equilib.*, 38 (1987) 245.
[4] C.H. Kang and S.I. Sandler, *Biotechnol. Bioeng.*, 32 (1988) 1158.
[5] Y.-L. Gao, Q.-H. Peng, Z.-C. Li and Y.-G. Li, *Fluid Phase Equilib.*, 63 (1991) 173.
[6] R.S. King, H.W. Blanch and J.M. Prausnitz, *AIChE J.*, 34 (1988) 1585.
[7] N.L. Abbott, D. Blankschtein and T.A. Hatton, *Macromolecules*, 24 (1991) 4334.
[8] C.A. Haynes, F.J. Benitez, H.W. Blanch and J.M. Prausnitz, *AIChE J.*, 39 (1993) 1539.
[9] Y. Guan, X.-Y. Wu, T.E. Treffry and T.H. Lilley, *Biotechnol. Bioeng.*, 40 (1992) 517.
[10] Y. Guan, T.E. Treffry and T.H. Lilley, *Bioseparation*, 4 (1993) in press.
[11] A.D. Diamond and J.T. Hsu, *AIChE J.*, 36 (1990) 1017.
[12] M. Setchenow, *Ann. Chim. Phys.*, 25 (1892) 226.
[13] H.L. Friedman, *J. Solution Chem.*, 1 (1972) 387.
[14] E.S. Vainerman, V.Yu. Ryashentsev and S.V. Rogozhin, *Solvent Extr. Ion Exch.*, 8 (1990) 361.
[15] A.D. Diamond and J.T. Hsu, in M.M. Ataai and S.K. Sikdar (Editors), *New Developments in Bioseparation (AIChE Symposium Series*, No. 290), American Institute of Chemical Engineers, New York, 1992, ch. 13.
[16] P.J. Flory, *Principles of Polymer Chemistry*, Cornell University Press, Ithaca, NY, 1953.
[17] Y. Guan, T.H. Lilley and T.E. Treffry, *J. Chem. Soc., Faraday Trans.*, 89 (1993) 4283.
[18] Y. Guan, T.H. Lilley and T.E. Treffry, *Macromolecules*, 26 (1993) 3971.
[19] Y. Hu and J.M. Prausnitz, *AIChE J.*, 35 (1988) 814.
[20] B.J. Alder, W.G. Hoover and D.A. Young, *J. Chem. Phys.*, 49 (1968) 3688.
[21] H.L. Weissberg, *J. Appl. Phys.*, 34 (1963) 2636.
[22] D. Forciniti, C.K. Hall and M.-R. Kula, *J. Biotechnol.*, 16 (1990) 279.
[23] R.H. Fowler and E.A. Guggenheim, *Statistical Thermodynamics*, Cambridge University Press, Cambridge, 1965.
[24] J. des Cloizeaux and G. Jannink, *Polymers in Solution: Their Modelling and Structure*, Clarendon Press, Oxford, 1990.
[25] D. Forciniti, C.K. Hall and M.-R. Kula, *Biotechnol. Bioeng.*, 38 (1991) 986.
[26] A.D. Diamond and J.T. Hsu, *Biotechnol. Techniq.*, 3 (1989) 119.
[27] P.-Å. Albertsson, *Partition of Cell Particles and Macromolecules*, Wiley, New York, 3rd ed., 1986.
[28] B.K. Kim, Y.-B. Ban and J.-D. Kim, *Korean J. Chem. Eng.*, 9 (1992) 219.
[29] Å. Sjöberg and G. Karlström, *Macromolecules*, 22 (1989) 1325.
[30] B.Yu. Zaslavsky, T.O. Bagirov, A.A. Borovskaya, N.D. Gulaeva, L.H. Miheeva, A.U. Mahmudov and M.N. Rodnikova, *Polymer*, 30 (1989) 2104.
[31] T.E. Treffry, T.H. Lilley and P.J. Cheek, in D. Fisher and I.A. Sutherland (Editors), *Separations Using Aqueous Phase Systems*, Plenum Press, London, 1989, p. 233.
[32] S.M. Snyder, K.D. Cole and D.C. Szlag, *J. Chem. Eng. Data*, 37 (1992) 268.
[33] X. Lei, A.D. Diamond and J.T. Hsu, *J. Chem. Eng. Data*, 35 (1990) 420.